

Supplementary Information

Constructing asymmetric covalent organic frameworks to facilitate photocatalytic hydrogen production

Jiaqi Li,^a Zhongliao Wang,^{b*} Yun Yang,^a Lijie Zhang,^a Jiajie Fan,^{c,d*} and Quanlong Xu^{a*}

^a*Wenzhou Key Lab of Advanced Energy Storage and Conversion, Zhejiang International Joint Laboratory of Optical Functional Materials, College of Chemistry and Materials Engineering, Wenzhou University, Wenzhou 325027, China*

^b*Anhui Key Laboratory of Energetic Materials, College of Physics and Electronic Information, Huaibei Normal University, Anhui, 235000, China*

^c*School of Materials Science and Engineering, Zhengzhou University, Zhengzhou 450001, China*

^d*Henan Zhongmei Electrical Co., Ltd. Pingdingshan, 467099, China*

* Corresponding authors.

E-mail addresses: wangzl@chnu.edu.cn (Z. Wang); fanjiajie@zzu.edu.cn (J. Fan); xuql@wzu.edu.cn (Q. Xu).

1. Experimental details

Materials

Benzo[1,2-b:3,4-b':5,6-b'']trithiophene-2,5,8-tricarbaldehyde (BTT) was purchased from Bide Pharmatech Co.,Ltd. Ascorbic acid (AA) was purchased from J & K Scientific. Methanol and Tetrahydrofuran (THF) were purchased from Wenzhou Jinshan Chemical Reagent Co., Ltd. Nafion D-520 dispersion was purchased from Alfa Aesar. The other reagents and solvents were purchased from Aladdin. All reagents were used without further purification.

Sample preparation

Preparation of BTTBD-COF: According to previous reports^[1], BTTBD-COF was prepared by solvothermal method. Benzo[1,2-b:3,4-b':5,6-b'']trithiophene-2,5,8-tricarbaldehyde (BTT, 19.8 mg, 0.06 mmol) and 4,4-biphenylenediamine (BD, 16.6 mg, 0.09 mmol) were dispersed into the mixture solvent containing o-dichlorobenzene (0.5 mL) and n-butanol (0.5 mL). After 15 minutes of ultrasonic treatment, 100 μ L of acetic acid (6 mol/L) aqueous solution was dropwise added under continuous ultrasound to obtain uniform dispersion. Then, it was degassed by three freeze pump-thaw cycles at 77 K (liquid nitrogen bath), sealed and heated to 120 °C for 3 days. The resulting precipitate was filtered, washed three times with tetrahydrofuran (THF) and methanol, and then vacuum dried at 80 °C for 12 hours to obtain a pale yellow powder denoted as BTTBD-COF.

Preparation of TpBD-COF

According to previous reports^[2], TpBD-COF was prepared by solvothermal method.

Specifically, 1,3,5-triformylphloroglucinol (Tp, 12.5 mg, 0.06 mmol) and 4,4'-biphenylenediamine (BD, 16.6 mg, 0.09 mmol) were dispersed into the mixture solvent containing o-dichlorobenzene (0.5 mL) and n-butanol (0.5 mL). After 15 minutes of ultrasonic treatment, 100 μ L of acetic acid (6 mol/L) aqueous solution was dropwise added under continuous ultrasound to obtain uniform dispersion. Then, it was degassed by three freeze pump-thaw cycles at 77 K (liquid nitrogen bath), sealed and heated to 120 °C for 3 days. The resulting precipitate was filtered, washed three times with tetrahydrofuran (THF) and methanol, and then vacuum dried at 80 °C for 12 hours to obtain red powder named as TpBD-COF.

Preparation of BTT-Tp-BD-COF

Three ternary COFs with different monomer ratios were prepared by the solvothermal method. During the specific sample preparation process, a certain proportion of 1,3,5-triformylphloroglucinol (Tp) and benzo[1,2-b:3,4-b':5,6-b'']trithiophene-2,5,8-tricarbaldehyde (BTT) were added in a Pyrex tube reactor, followed by the addition of 4,4'-biphenylenediamine (BD, 16.6 mg, 0.09 mmol). Then, o-Dichlorobenzene (0.5 mL) and n-butanol (0.5 mL) were added as solvents. After ultrasonic treatment for 15 minutes, 100 μ L of acetic acid aqueous solution (6 mol/L) was introduced under continuous ultrasonication to obtain a homogeneous dispersion. Then, the mixture was degassed by three freeze-pump-thaw cycles at 77 K (liquid nitrogen bath), sealed, and heated at 120 °C for 3 days. The resulting precipitate was filtered, washed with tetrahydrofuran (THF) and methanol three times, and then dried under vacuum at 80 °C for 12 hours to obtain orange powders. When the usage of Tp and

BTT were 1.3 mg (0.006 mmol) and 17.8 mg (0.054 mmol), the collected sample was named $\text{BTT}_{0.9}\text{Tp}_{0.1}\text{BD-COF}$. While, Tp (2.0 mg, 0.009 mmol) and BTT (16.8 mg, 0.051 mmol) for $\text{BTT}_{0.85}\text{Tp}_{0.15}\text{BD-COF}$, and Tp (2.6 mg, 0.012 mmol) and BTT (15.8 mg, 0.048 mmol) for $\text{BTT}_{0.8}\text{Tp}_{0.2}\text{BD-COF}$.

2. Characterization

The microstructure of the prepared samples was observed by field emission scanning electron microscopy (FE-SEM, Sigma 300, Germany) and transmission electron microscopy (TEM, JEOL, JEM-2100F, Japan). The crystalline phases of the samples were collected by powder X-ray diffraction (XRD, SmartLab, Japan) in the 2θ range from 2° to 40° . Fourier transform infrared spectroscopy (FT-IR) was measured on Spectrum 3 (PerkinElmer, USA). Ultraviolet-visible diffuse reflectance spectroscopy (UV-Vis DRS) was measured on (Shimadzu 3600, Japan) with BaSO_4 as a reference. X-ray photoelectron spectroscopy (XPS) was measured using PHI 5000 VP III (ULVAC-PHI, Japan). In the in-situ XPS measurement process, a monochromatic laser ($\lambda = 405 \text{ nm}$) was introduced as the light source, and the power was adjusted to 100 mW. Nitrogen adsorption-desorption isotherms were conducted on ASAP 2020 (USA), which were measured at 77 K. The sample was vacuum-degassed at 150°C for 10 hours before measurement. Photoluminescence (PL), time-resolved photoluminescence decay spectrum (TR-PL), and temperature-dependent photoluminescence spectrum were obtained on the combined fluorescence equipment spectrometer (including liquid nitrogen cryostat) (Orient KOJI, China). The contact angle was measured on K100 (KRUSS, Germany) instrument.

Photoelectrochemical measurement

The electrochemical impedance spectroscopy (EIS), transient photocurrent response and Mott-Schottky (M-S) were tested on an electrochemical workstation (CHI760E) using a standard three-electrode system. The Ag/AgCl electrode, platinum electrode, and fluorine-doped tin oxide (FTO) coated with the prepared sample were used as reference electrode, counter electrode, and working electrode, respectively. 0.5 mol/L Na₂SO₄ solution was used as the electrolyte. As for the preparation of working electrode, 5 mg photocatalyst was homogenously dispersed in 5 % (mass fraction) Nafion (40 μL), ethanol (250 μL) and ethylene glycol (250 μL) through ultrasonic treatment for 30 minutes. Then, the above mixture (40 μL) was dropped on the FTO glass surface, followed with drying at 80 °C for 2 hours. Electrochemical impedance spectroscopy (EIS) was measured at frequency ranging from 1 to 100 kHz. The M-S curves were measured at fixed frequency of 1, 2, and 3 kHz. The photocurrent time (I-t) curve was tested under intermittent illumination.

Photocatalytic performance measurement

The photocatalytic hydrogen production performance of the prepared samples was determined by an online system (Labsolar-6A, Beijing Perfect light, China). A 300 W Xe lamp (PLS-SXE300D, Beijing Perfect light, China) was used as the light source, which was equipped with a cutoff filter with wavelength of 420 nm. During the test, 10 mg of the prepared photocatalyst was dispersed into 100 mL of ascorbic acid (AA, 0.05 mol/L) solution serving as a sacrificial agent, and 3 % (mass fraction) of platinum was loaded by in-situ photoreduction method as a co-catalyst for 30

minutes. To exclude the thermal effect, the reaction system was maintained at 6 °C. The hydrogen yield was determined using a gas chromatograph (GC, Agilent 7890A, USA) equipped with a thermal conductivity detector (TCD). In addition, a cycle test was performed to study the stability of the sample. Besides, the apparent quantum efficiency (AQE) at different wavelengths of 450 nm, 500 nm, 550 nm, and 600 nm was measured. The corresponding photon flux densities were detected as 2.3, 4.45, 9.61, and 1.82 milliwatts per square centimeter, respectively. These data were obtained by the optical power meter (Newport Corporation, 1918-R type). AQE was calculated using the following formula:

$$\text{AQE(\%)} = \frac{2 \times \text{number of hydrogen}}{\text{number of incident photons}} \times 100\%$$

3. Computational detail

Spin-polarized DFT calculations were conducted through the Vienna ab initio Simulation Package (VASP) with the projector augment wave method^{[3],[4]}. Generalized gradient approximation of the Perdew-Burke-Ernzerhof (PBE) functional was used as the exchange-correlation functional^[5]. The Brillouin zone was sampled with gamma points for surface calculation^[6]. The cutoff energy was set as 500 eV, and structure relaxation was performed until the convergence criteria of energy and force reached 1×10^{-5} eV and 0.02 eV \AA^{-1} , respectively. A vacuum layer of 15 Å was constructed to eliminate interactions between periodic structures of surface models. The van der Waals (vdW) interaction was amended by the zero damping DFT-D3 method of Grimme^[7].

Table S1 The elementary analysis of BTTBD, BTT_{0.9}Tp_{0.1}BD, BTT_{0.85}Tp_{0.15}BD, and BTT_{0.8}Tp_{0.2}BD.

Samples	N (at%)	C (at%)	S (at%)	S/N
BTTBD-COF	0.50	5.57	0.47	1
BTT _{0.9} Tp _{0.1} BD-COF	0.50	5.50	0.42	0.90
BTT _{0.85} Tp _{0.15} BD-COF	0.50	5.53	0.40	0.84
BTT _{0.8} Tp _{0.2} BD-COF	0.50	5.39	0.38	0.80

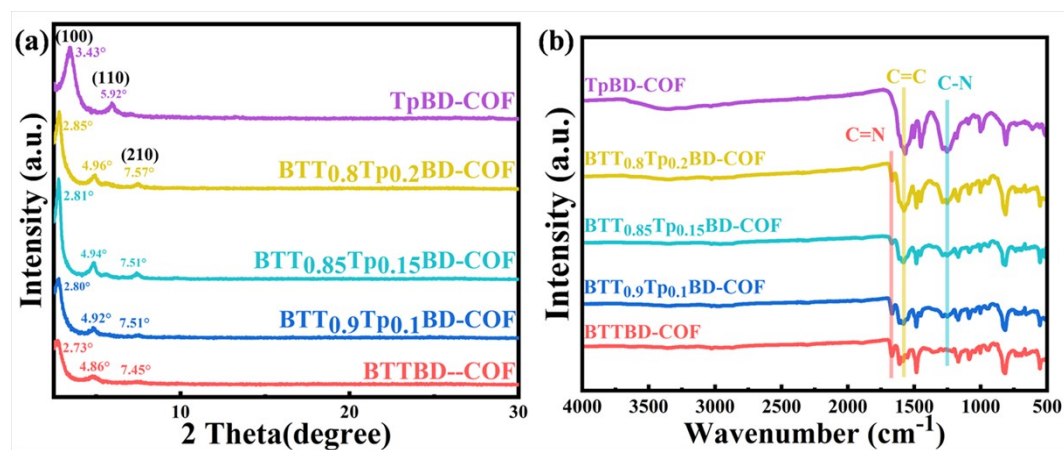


Fig. S1 PXRD patterns (a) and Fourier transform infrared (FT-IR) spectra (b) of the prepared samples.

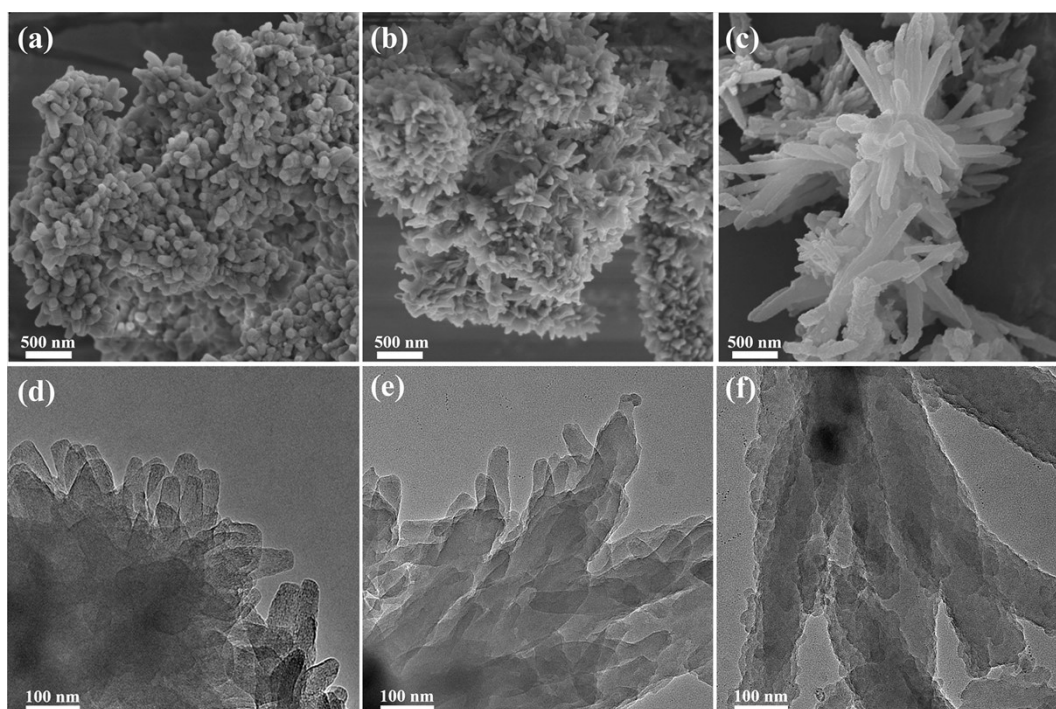


Fig. S2 SEM and TEM images of BTTBD-COF (a,d), BTT_{0.85}Tp_{0.15}BD-COF (b,e), and TpBD-COF (c,f).

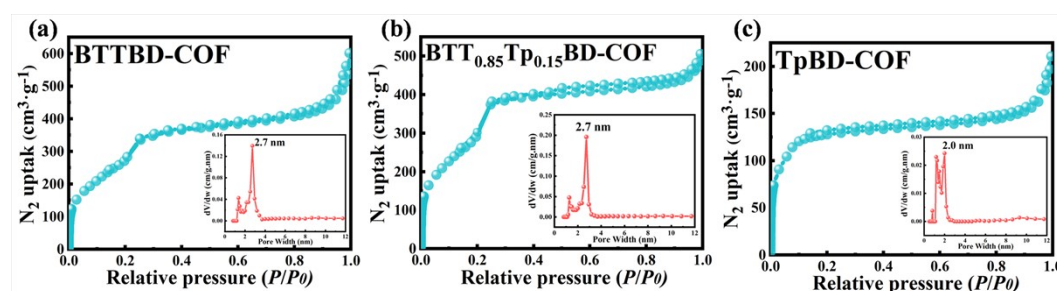


Fig. S3 N₂ adsorption-desorption isotherms of BTTBD-COF (a), BTT_{0.85}Tp_{0.15}BD-COF (b), and TpBD-COF (c).

Table S2 Textural properties of BTTBD, BTT_{0.85}Tp_{0.15}BD, and TpBD.

Samples	S _{BET} (m ² /g)	Average pore size (nm)	Pore volume (cm ³ /g)
BTTBD-COF	1193.6	2.7	0.78
BTT _{0.85} Tp _{0.15} BD-COF	1347.4	2.7	0.78
TpBD-COF	415.5	2.0	0.32

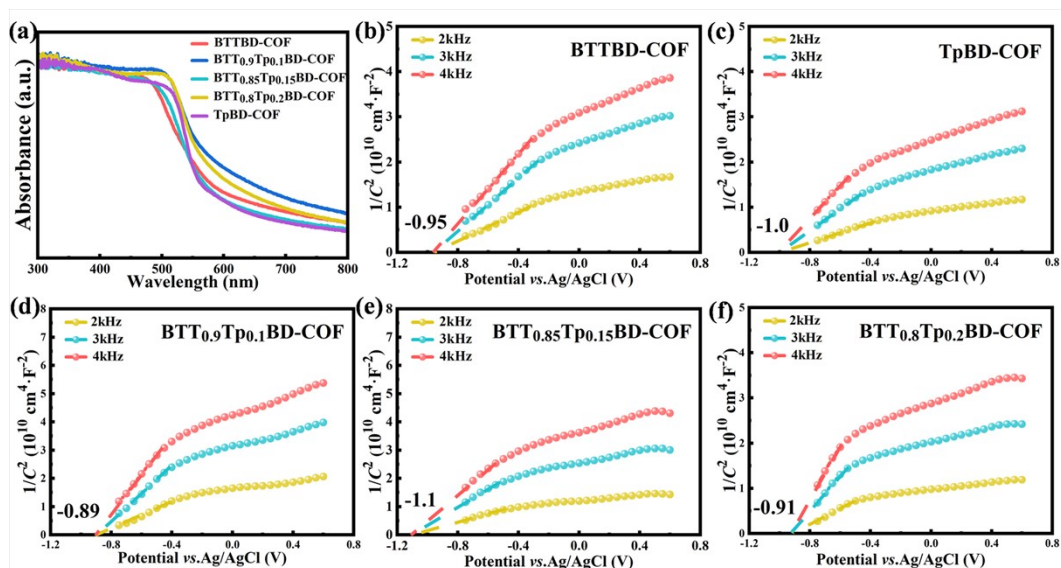


Fig. S4 (a) UV-Vis DRS spectra of the prepared samples. Mott-Schottky plots of BTTBD-COF (b), TpBD-COF (c), BTT_{0.9}Tp_{0.1}BD-COF (d), BTT_{0.85}Tp_{0.15}BD-COF (e) and BTT_{0.8}Tp_{0.2}BD-COF (f) at 1–3 kHz.

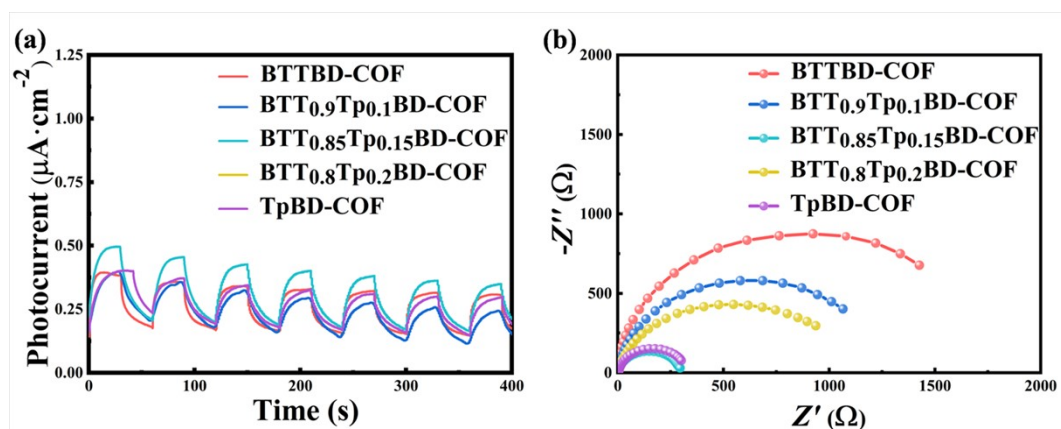


Fig. S5 (a) Transient photocurrent spectra and (b) electrochemical impedance spectroscopy (EIS) of the prepared samples.

Table S3 Comparison of photocatalytic hydrogen evolution performance over TpBD-COF-based photocatalysts.

Samples	H ₂ Evolution Rate (mmol·g ⁻¹ ·h ⁻¹)	AQE	Light Source	Co-catalyst	Refs
TpBD COF@ZIS-10	2.304	5.02% (420 nm)	300 W Xe lamp, > 420 nm	Pt	1
8-MoS ₂ /TpBD-COF	2.97	0.44% (420 nm)	300 W Xe lamp, > 420 nm	MoS ₂	8
NiS ₃ -BD	3.84	0.24% (420 nm)	300 W Xe lamp, > 420 nm	NiS	9
CdS-1%COF	15.1	0.3% (450 nm)	300 W Xe lamp, > 420 nm	Pt	10
2% AuNBs/TpBD-COF	6.27	0.58% (420 nm)	300 W Xe lamp, > 420 nm	Pt	11
TpBd-2D	9.4	8.03% (420 nm)	300 W Xe lamp, > 420 nm	Pt	12
BTT _{0.85} Tp _{0.15} BD-COF	7.62	0.48% (450 nm)	300 W Xe lamp, > 420 nm	Pt	This work

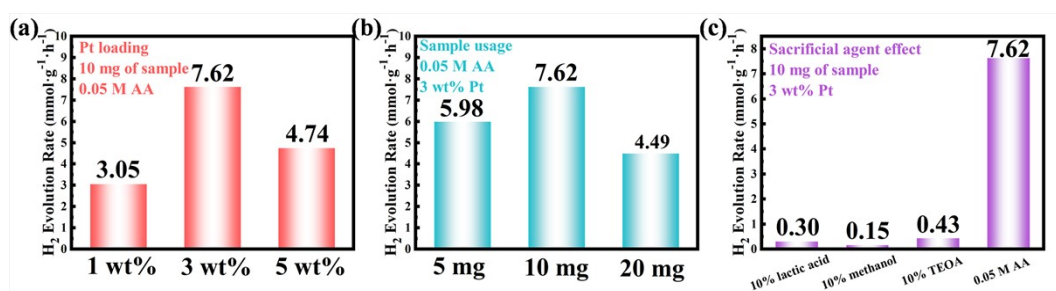


Fig. S6 Photocatalytic H₂ evolution rate of BTT_{0.85}Tp_{0.15}BD-COF under different conditions.

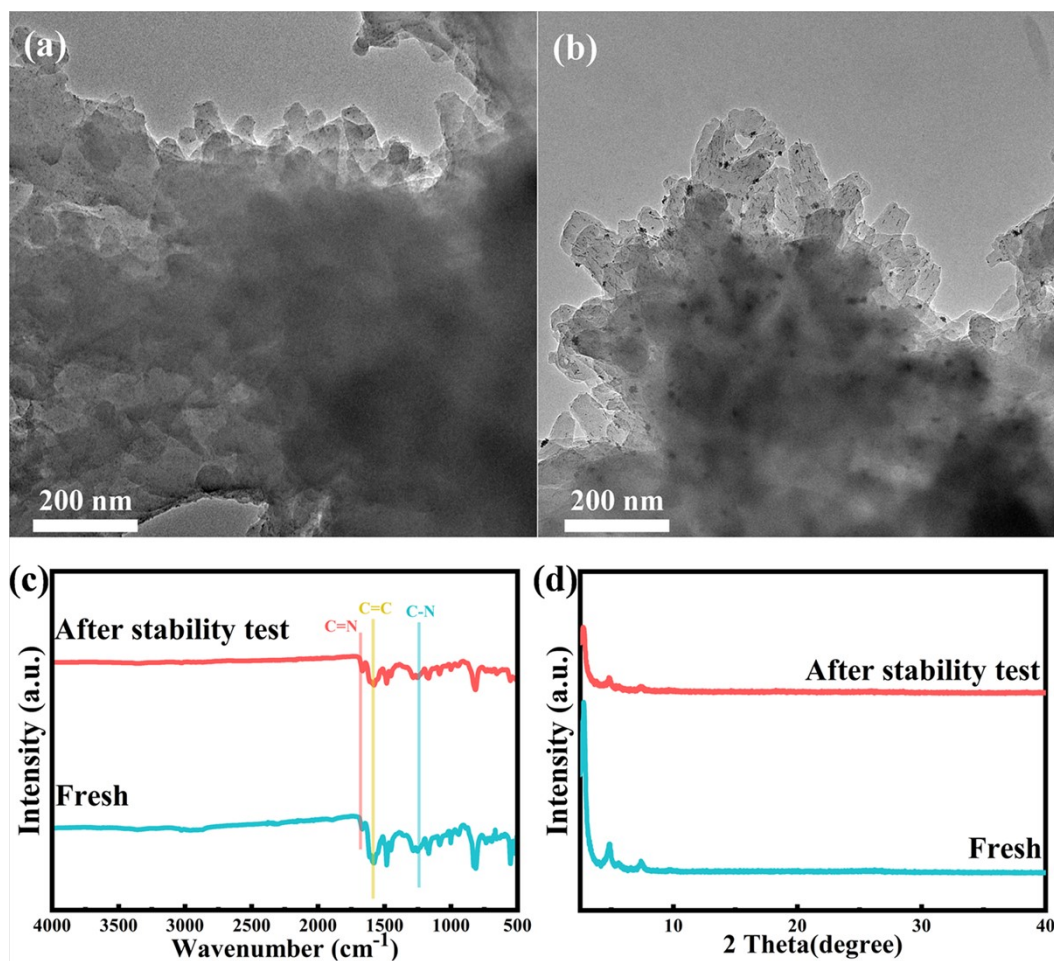


Fig. S7 TEM images of the fresh Pt loaded on BTT_{0.85}Tp_{0.15}BD-COF (a) and BTT_{0.85}Tp_{0.15}BD-COF after cycle test (b), FT-IR spectra (c) and XRD pattern (d) of BTT_{0.85}Tp_{0.15}BD-COF before and after cycle test.

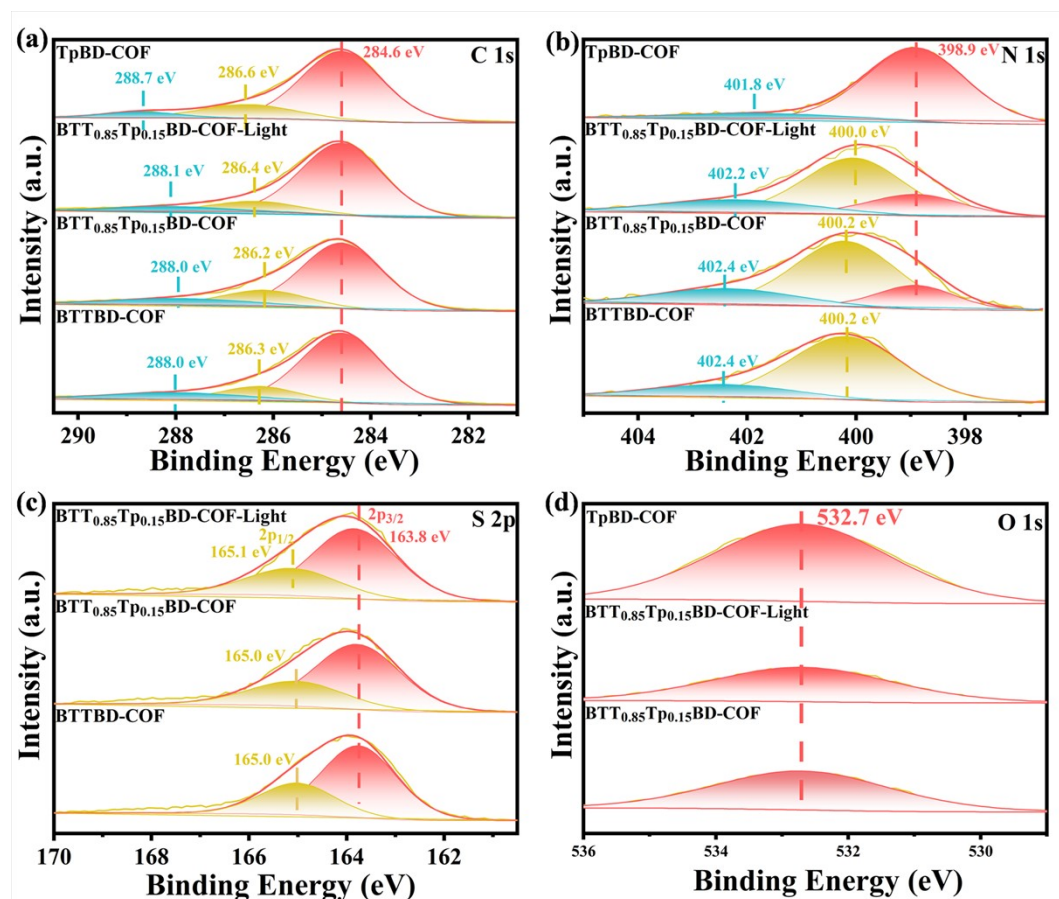


Fig. S8 The high-resolution XPS spectra of BTTBD-COF, BTT_{0.85}Tp_{0.15}BD-COF, and TpBD-COF: (a) C 1s, (b) N 1s, (c) S 2p, and (d) O 1s. In-situ XPS characterization was performed under monochromatic light ($\lambda=405$ nm).

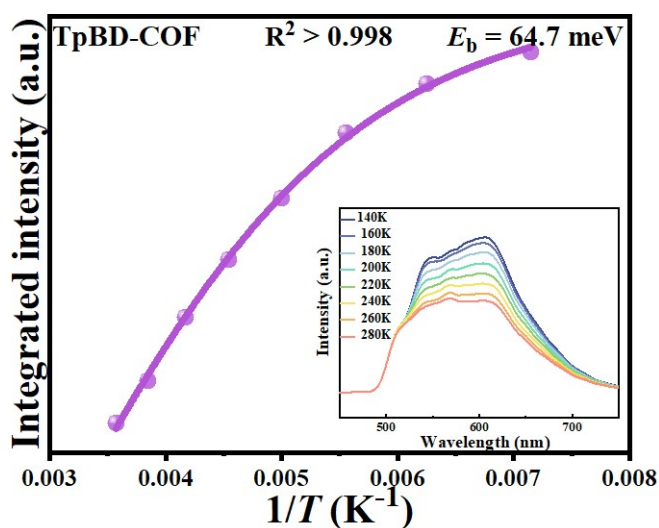


Fig. S9 Temperature-dependent fluorescence spectra of TpBD-COF.

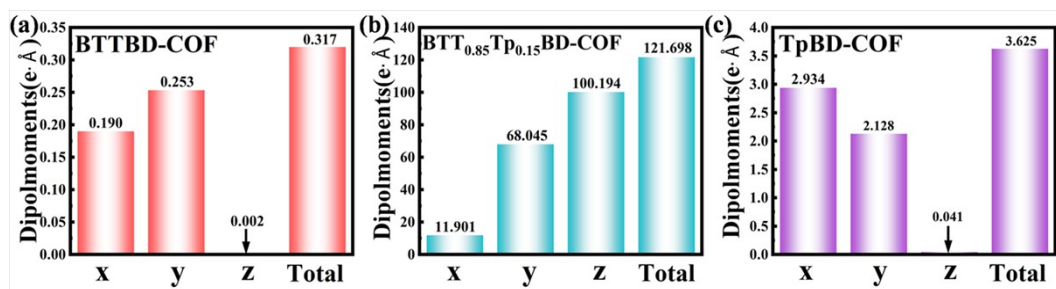


Fig. S10 The dipole moment of (a) BTTBD-COF, (b) BTT_{0.85}Tp_{0.15}BD-COF, (c) TpBD-COF.

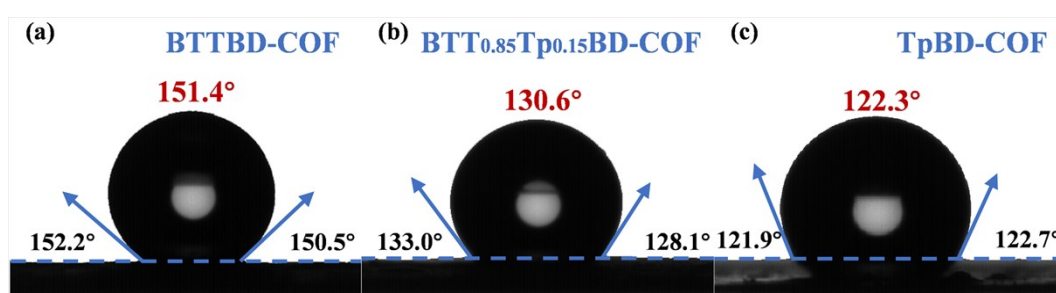


Fig. S11 Contact angle of BTTBD-COF (a), BTT_{0.85}Tp_{0.15}BD-COF (b), TpBD-COF.

The polarity of Tp and BTT units are calculated as follows:

$$\begin{aligned} \mu_{Tp} &= (\mu_{-OH(Ar)} \times n_{-OH} + \mu_{-CHO(Ar)} \times n_{-CHO}) \times \alpha \\ &= (5.6 \times 3 + 2.3 \times 3) \times 0.12 \\ &= 2.84 \text{ Debye} \end{aligned}$$

$$\begin{aligned} \mu_{BTT} &= (\mu_{-CHO(Ar)} \times n_{-CHO}) \times \alpha \\ &= (2.3 \times 3) \times 0.1 \\ &= 0.69 \text{ Debye} \end{aligned}$$

Reference

- [1] S. Bao, Q. Tan, S. Wang, J. Guo, K. Lv, SAC Carabineiro, L. Wen, *Applied Catalysis B: Environmental*, 2023, **330**, 122624.
- [2] C. Qin, Y. Yang, X. Wu, L. Chen, Z. Liu, L. Tang, L. Lyu, D. Huang, D. Wang, C. Zhang, X. Yuan, *Nat. Commun.*, 2023, **14**, 6740.

- [3] G. Kresse, D. Joubert, *Phys. Rev. B*, 1999, **59**, 1758–1775.
- [4] P. E. Blöchl, *Phys. Rev. B* 1994, **50**, 17953–17979.
- [5] J. P. Perdew, K. Burke, M. Ernzerhof, *Phys. Rev. Lett.* 1996, **77**, 3865–3868.
- [6] V. Wang, N. Xu, J. Liu, G. Tang, W. Geng, *Computer Physics Communications*, 2021, **267**, 108033.
- [7] S. Grimme, S. Ehrlich, L. Goerigk, *J. Comput. Chem.*, 2011, **32**, 1456–1465.
- [8] H. Yang, L. Wang, Y. Xia, X. Li, J. Yan and L. Wen, *Dalton Trans.*, 2025, **54**, 14790.
- [9] H. Zhang, Z. Lin and J. Guo, *RSC Adv.*, 2022, **12**, 14932-14938.
- [10] G. Sun, J. Zhang, B. Cheng, H. Yu, J. Yu, J. Xu. *Chem Eng J.* 2023, **476**, 146818.
- [11] Y. Deng, Y. Chen, L. Zhang, H. Jin, Y. Yang, Q. Xu, S. Wang, *Acta Phys. -Chim. Sin.*, 2025, doi: 10.1016/j.actphy.2025.100193.
- [12] Y. Wei, Z. Su, Y. Li, F. Wang, W. Yan, Y. Gao, Z. Li, Y. Chen and J. Xu, *Chem. Commun.*, 2025, **61**, 10343-10346.